Lasers in Manufacturing Conference 2021

Superhydrophobic surfaces using ultra-short pulse structuring of thin metals

Fabian Schaefer[a,*], Simon Ruck[a], Max-Jonathan Kleefoot[a], Wadim Schulz[b], Florian Köhn[b], Joachim Albrecht[b], Harald Riegel[a]

[a]*Laser-Application Center LAC, Aalen University, Beethovenstraße 1, 73430 Aalen, Germany*
[b]*Insitute for Innovative SurfacesFINO, Aalen University, Beethovenstraße 1, 73430 Aalen, Germany*

Abstract

Fabrication of superhydrophobic surfaces induced by ultra-short-pulse lasers is a hotspot of surface studies. We report a way of generating superhydrophobic surfaces on stainless steel (304S15). The method for fabricating this water-repellent surface is to microstructure by irradiating with ultra-short-pulses.
Contact angle measurements were used to investigate the wettability of the surface in relation to the laser parameters (laser fluence and scan line separation). The steady contact angle was investigated in the range of 140°. Investigations with optical measuring methods (white light interferometer) displays the structures of the surfaces. The generated surface shows hierarchical structures with nano and micro roughness similar to a lotus leaf. In further experiments, different materials shall be sputtered to obtain a thin stainless steel layer. Subsequent laser structuring should produce a functional surface with water repellent properties

Keywords: superhydrophobic surfaces; laser structuring; ultra short pulse; sputtering; stainless steel

1. Introduction

This proceeding deals with the phenomenon of different wetting properties on structured stainless steel surfaces. It is known that rough and porous surfaces have different wetting properties than the smooth surface of the same material. A possibility is explained which ensures that stainless steel surfaces develop water-

* Corresponding author Tel.: +49 15206435225.
E-mail address: fabian.schaefer@studmail.htw-aalen.de.

repellent properties. Laser structuring with ultra-short pulses can systematically roughen the surface, which after an aging process exhibits almost superhydrophobicity.

Metals usually show a strong wettability for water and oil, as well as other liquids. In this proceeding a possibility is shown to give stainless steel (more precisely 1.4301 / 304S15 / X5CrNi-1810) specific wetting properties by processing with ultra-short laser pulses (USP). Functionalized surfaces like these belong to the well-discussed area of surface research besides biomimetic surfaces and other applications [Bhushan, B. 2018; Ghasemlou, M. 2019].

The key advantage of USP processing is the possible cold ablation of material. Heat diffusion plays a minor role, and the machined material immediately changes from the solid to the gaseous aggregate state (sublimation). Due to this minimal thermal and mechanical damage zone (low heat affected zone, few distortions, few cracks, few debris), it is possible to work with a high degree of precision [Nolte, S. 1999]. According to [Vorobyev, A.Y. 2013] surface structures in the sub micrometer range can be achieved. Nevertheless, it should be mentioned that a deposition of nanoparticles [Gurera, D. 2018] can also take place next to the machined area.

USP processing allows to create regular deterministic structures as well as stochastic structures. So-called laser-induced-periodic surface structures (LIPSS) [Müller, F. A. 2016] are gaining more and more interest in research and development, as they have a great potential to create diverse surfaces for various technical applications [Müller, F. A. 2016]. The properties of LIPSS depend on the wavelength λ, the laser fluence F, the optical properties and the number of laser pulses N incident on the surface [Wu, P.H. 2011].

Superhydrophobic surfaces occur very frequently in nature and are created via different surface properties. What all liquid-repellent surfaces have in common is that they have a hierarchical structure and the lowest possible surface free energy (SFE). The surface free energy is defined as the work that would have to be expended to increase the surface area of a solid phase. Simply put, the work required to wet the surface of a material with a liquid [DIN EN 828]. The surface thus has a certain waviness in the micrometer range, which is superimposed by a roughness in the nanometer range [Müller, F. A. 2016]. The superimposed roughness's led to a Wenzel or also Cassie-Baxter state of the surface. Wenzel [Wenzel, R.N. 1936] and Cassie-Baxter [Cassie, A.B.D., Baxter, S. 1944] describe wetting models for different surfaces. The Robert-Wenzel model describes the change in contact angle as a function of roughness. Cassie-Baxter´s model reports the wettability for porous surfaces.

Van Duon Ta [Ta, V.D. 2016] have shown that stainless steel, 304S15, develops water-repellent properties by laser material processing and aging. Laser-textured samples with different scan line spacings and altered fluence achieve contact angles to water up to 154° with a hysteresis of 4°. A hysteresis of less than 10° ensures that the droplet can glide over the surface [Wang, S. 2007].

2. Experimental set up

The experiments were performed with a VaryDisk Femto 100 (Dausinger and Gießen, Germany) ultra-short-pulsed laser system. It has a tunable pulse duration in the range of 600 fs – 18 ns at center wavelength of 1030 nm and a repetition rate from single pulses up to 1 MHz. For our experiments, the laser system is optimized to work with 6 W average laser power at pulse repetition of 200 kHz. The VaryDisk Femto 100 is integrated in a high precision 5-Axis machine, microcut UKP (LLT GmbH, Ilmenau Germany) to enable 3D laser micro machining. Therefore, the laser beam is guided by an optical rail system into the machine. An exelliSCAN14 (SCANlab, Puchheim Germany) galvo scanner system and F-a tele centric F-theta lens guides the laser beam over the work piece surface.

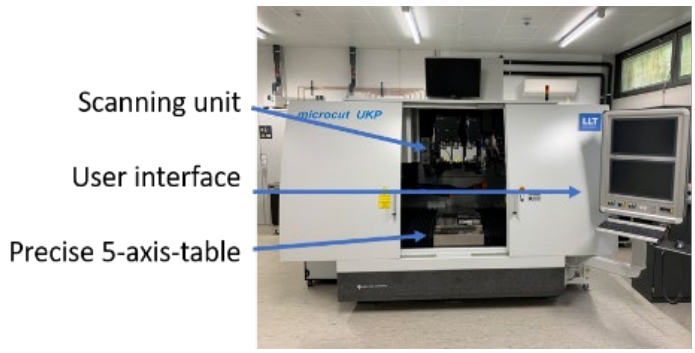

Fig. 1. Experimental set up with laser system and precise 5-axis-machine

The samples have a dimension of 15 mm * 15 mm with a thickness of 4 mm and made of stainless steel (1.4301, X5CrNi18-10) with 18 % Chromium and 10 % Nickel. Due to its high corrosion resistance and good processing properties, this austenitic chromium-nickel steel is used in many fields. Its hardness is less than or equal to 215 HB and has an $Rp_{0.2}$ greater than or equal to 190 MPa [Deutsche Edelstahlwerke, 2015].

Before laser structuring with USP the samples were grinded and polished to generate a smooth surface. The surface structure was determined by a ZYGO ZeGage (AMETEK Germany GmbH, Germany) white light interferometer (WLI). The roughness of the surface was quantified through the Ra-value as the average peak-to-valley height (arithmetic average of the sums of the deviation from the medium profile over the measured length).

After the characterization of the polished surfaces, the ultra-short-pulsed laser ablation experiments were performed. The aim of the laser structuring was a grid pattern with different scan line separations. The scan line separation indicates the distance between two processing laser lines. Every laser parameter was kept constant except the scan line separation. The varied scan line separation results in different degrees of structured surfaces. Figure 2 shows a sketch of the laser structuring process for a big scan line separation and a small scan line separation:

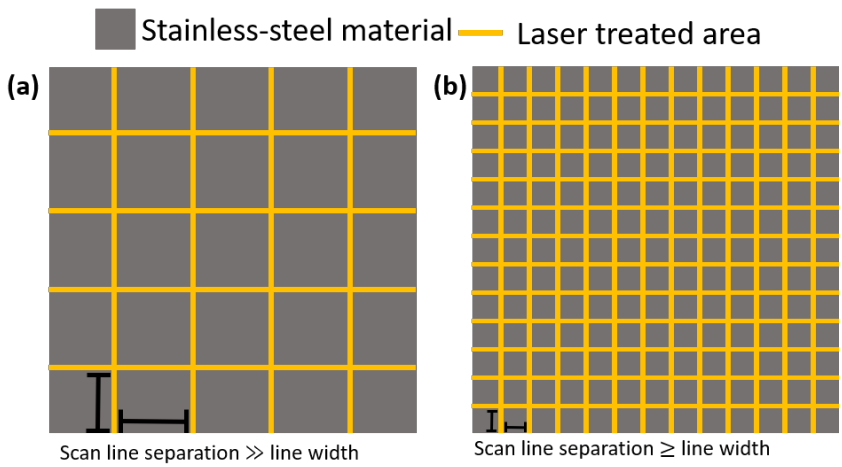

Fig. 2. Sketch of different scan line separations (a) big scan line separation, (b) small scan line separation, a smaller scan line separation resulting in more laser lines on the stainless-steel surface

Table 1 lists the parameters for the ablation study. All experiments were run with constant pulse overlap PO of 67 % to avoid the influence of incubation effects on the ablation results [Neuenschwander et al. 2012]. Scan velocity v_{scan} and the focal diameter of d_f = 18 µm kept constant, which resulted in the same number of pulses per dot – *N* = constant. Each line was did with 28 repetitions.

Table 1. Laser parameter for our experiment – laser structuring of stainless steel

parameter	abbreviation	value	unit
Laser power	P	6	W
Focal diameter	df	18	µm
Scanning speed	v_{scan}	1,2	m/s
Repetition rate	f_{rep}	200	kHz
Pulse duration	Pd	600	fs
Energy per Pulse	E_p	2.5 - 50	µJ
Pulse overlap	PO	67	%
Fluence	F	11,79	J/cm²
Passes per line	Pl	28	-

Finally, the wetting properties of the laser-structured stainless steel samples were measured with a contact angle meter - Drop Shape Analyzer 100 (Krüss Scientific, KRÜSS GmbH Hamburg, Germany) [Drop Shape Analyzer, 2017]. The contact angles of water against the laser structured surface after exposure to laboratory atmosphere for a various time of aging were determined. The liquid droplet volume is set to 5 µl. Figure 3 shows a sketch of a water droplet of the laser structured samples with two different scan line separations:

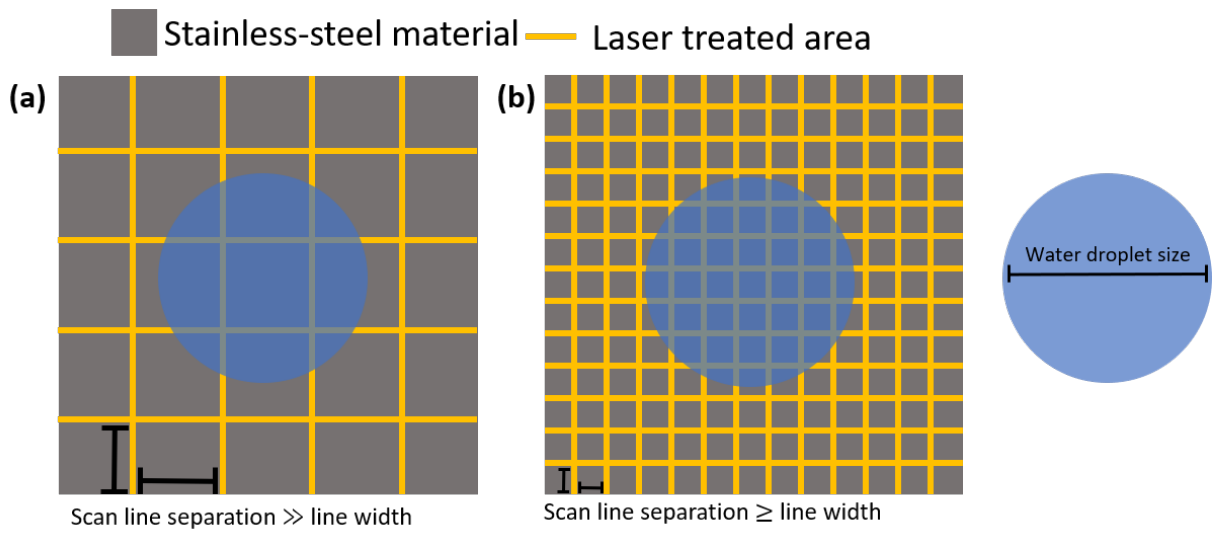

Fig. 3. Sketch of the ratio between a water droplet and the line width in relation to the scan line separation. (a) less laser lines under the water droplet, (b) more laser lines under the water droplet

Table 2. Ratio between droplet size of the test liquid in relation to the number of laser lines under the droplet

Scan line separation [µm]	Possible laser lines under a liquid drop	Ratio droplet size/laser lines
30	38	0.040
40	32	0.034
50	27	0.028
100	16	0.017
150	11	0.012
200	9	0.009
400	5	0.005
600	4	0.004
800	3	0.003

Table 2 and Figure 3 show for a constant droplet volume, that the number of laser lines under the liquid droplet decreases with increasing scan line separation. At lower scan line separation, there are more laser lines under the liquid droplet. The diameter of a 5 µl water drop is 1900 µm on the polished stainless steel surface. Thus, with a scan line separation of 800 µm, there can be 3 crossed lines under a drop. Conversely, at the smallest scan line separation of 30 µm, there are approx. 38 crossed lines under the drop.

Fig. 4. Drop Shape Analyzer 100 – picture from the user manual [Drop Shape Analyzer, 2017]

To summarize our approach: With an increasing scan line separation and constant focal diameter d_f and constant scan velocity v_{scan} the processed area becomes smaller. A large scan line separation thus provides a less structured area compared to a very narrow scan line separation, which results in a high structured area.

According to the models of Wenzel and Cassie-Baxter for rough and porous surfaces, we expect different wetting properties for smaller scan line separations than for the polished initial surface.

3. Results and discussion

Figure 5 displays white light interferometer images of the different laser structured samples with varied scan line separations (a)-(i). The recorded measurement area of the white light interferometer images is 800 µm by 800 µm. As the scan line separation of the samples increases (30 µm - 800 µm), the number of lines in the measurement area decreases. The line width is overall constant at 20 µm.

The initial roughness's of the polished stainless steel samples were Ra = 2.73 nm +/- 0.27 nm. After laser structuring, the overall roughness of the samples increased. A smaller scan line separation resulted in higher roughness values. Figure 5 (a) shows a roughness of Ra = 5.72 µm compared to Figure 5 (g) with a roughness of Ra = 1.38 µm. Interestingly, no linear behavior is evident. Figure 5 (h) and Figure 5 (i) with the largest scan line separations show higher Ra values than Figure 5 (g). This behavior was not expected. Probably, increases at the trenches lead to increased Ra values, which do not coincide with reality.

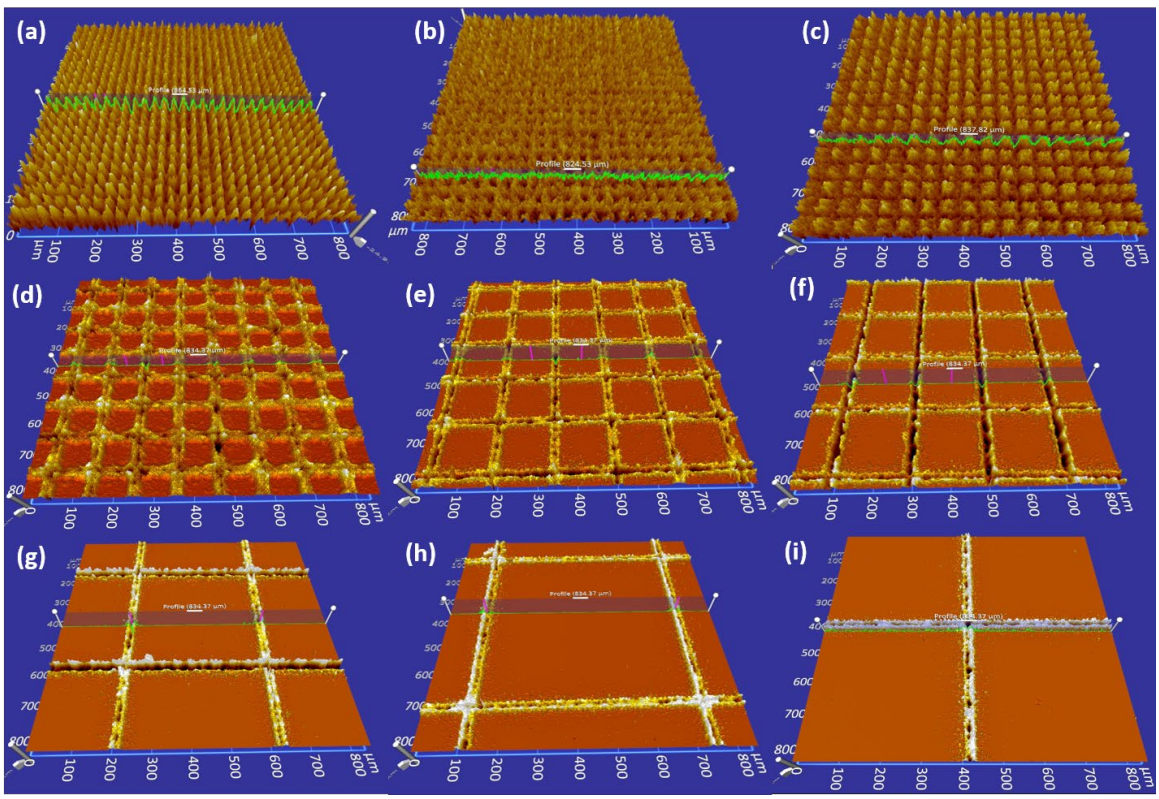

Fig. 5. White light interferometer images of laser structured stainless steel samples with different scan line separations: (a) 30 µm scan line separation – Ra: 5.72 µm (b) 40 µm scan line separation – Ra: 2.04 µm (c) 50 µm scan line separation – Ra: 5.01 µm (d) 100 µm scan line separation – Ra: 3.47 µm (e) 150 µm scan line separation – Ra: 3.80 µm (f) 200 µm scan line separation – Ra: 2.65 µm (g) 400 µm scan line separation – Ra: 1.38 µm (h) 600 µm scan line separation 2.65 µm (i) 800 µm scan line separation – Ra: 2.90µm

At a scan line spacing of 100 to 800 µm, picture (d)-(i), yellow edges can be seen next to the lines on closer inspection. These could be throw-ups of molten and re-solidified metal. This could indicate some thermal influence through the laser process into the sample. USP processing should minimize this effect as much as possible.

Figure 6 shows the contact angles of water against the laser structured surface after exposure to laboratory atmosphere for 21 days. The scan line separation increases form (a) to (i), respectively from 30 µm to 800 µm scan line separation.

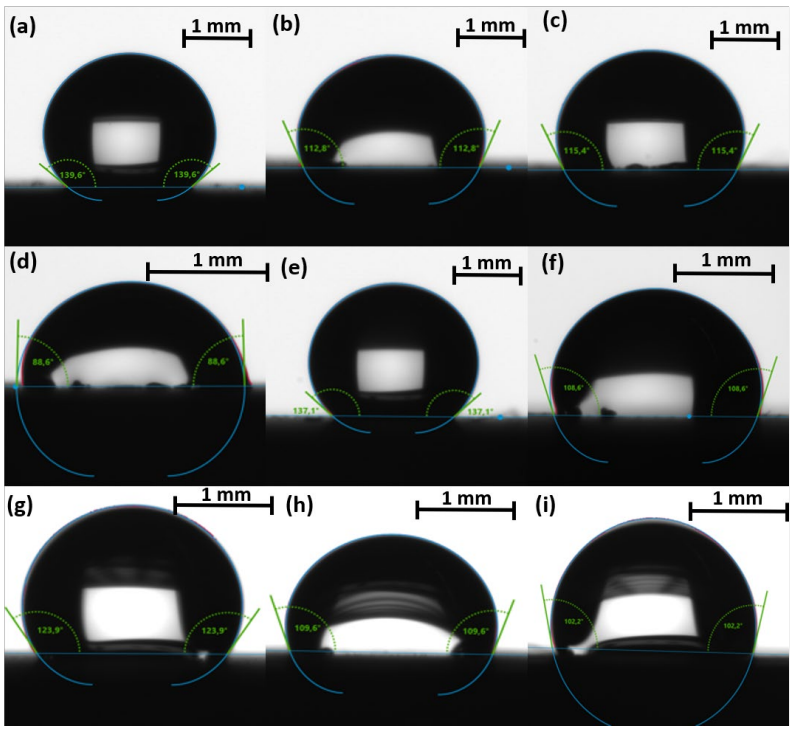

Fig. 6. Measured contact angles with DSA100 of water of laser structured stainless steel samples after 21 days exposed to laboratory atmosphere: (a) 30 µm scan line separation – Θ = 139.6° (b) 40 µm scan line separation – Θ = 112.8° (c) 50 µm scan line separation – Θ = 115.4° (d) 100 µm scan line separation – Θ = 86.6° (e) 150 µm scan line separation – Θ = 137.1° (f) 200 µm scan line separation – Θ = 108.6° (g) 400 µm scan line separation – Θ = 123.9° (h) 600 µm scan line separation Θ = 109.6° (i) 800 µm scan line separation – Θ = 102.2°

The highest contact angles were obtained with a scan line separation of (a) 30µm, Θ = 139.6° and (e) 150µm Θ = 137.1°. Larger scan line separation led to contact angles against water in the range between 110° (600 µm) and 102° (800 µm).

Figure 7 shows a close up of a 5 µl water droplet on a laser structured surface with a scan line separation of 150 µm. The droplet forms almost a sphere but sticks to the surface and does not slide if the sample is tilted.

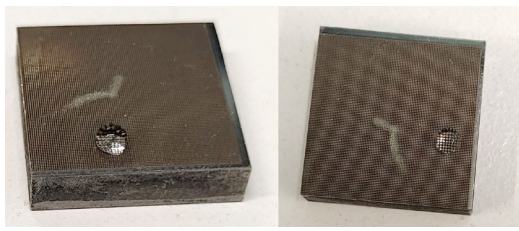

Fig.7. A water droplet of 5 µl on the sample with 150 µm scanline separation. The water droplet forms a sphere on the laser structured surface.

Figure 8 shows the achievable contact angles for water after 21 days of aging in laboratory atmosphere. The scan line separation in µm is plotted on the x-axis and the contact angle on the y-axis. A scan line separation of 30 µm and 150 µm achieve the highest contact angles. Between 50 µm and 150 µm the contact angle decreases before it increases again. As the scan line separation increases (>200 µm), the contact angle remains in the range between 100 and 120°.

According to [van Ta, D. 2016] the highest contact angles can be achieved in the range of 30 µm to 150 µm after 15 days of ageing without any decrease. One difference here could be a different fluence of 36 J/cm² compared to 11.8 J/cm².

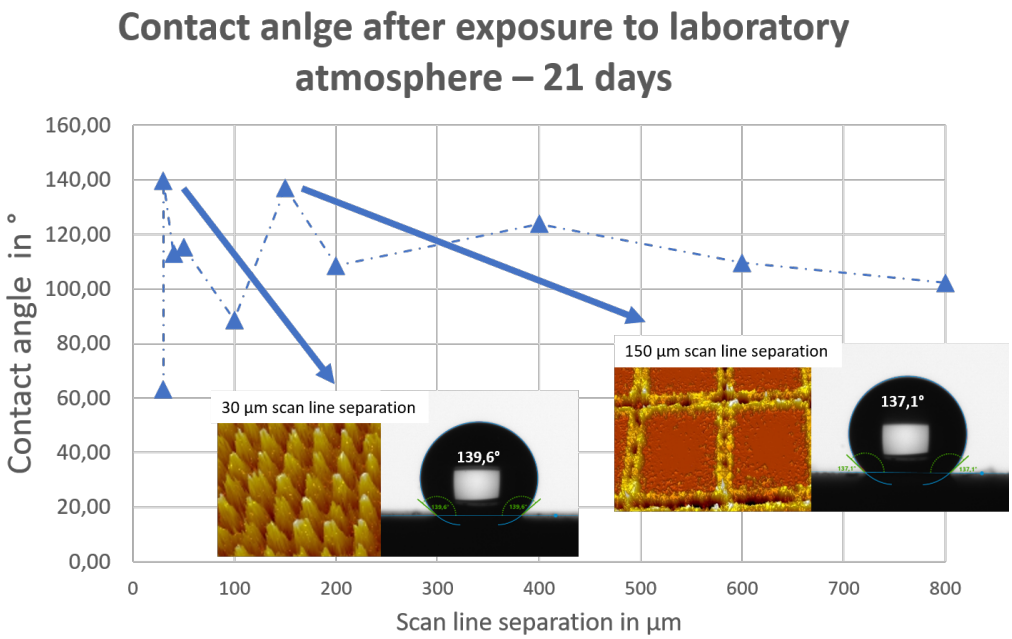

Fig. 8. Water contact angle in relation to scan line separation after 21 days exposure to laboratory atmosphere

Figure 9 illustrates the influence of exposure to laboratory atmosphere in relation to the scan line separation for the formation of a water-repellent surface on the stainless-steel samples. The y-axis shows the contact angle, the x-axis represents the aging time in days. With increasing ageing, the contact angle increases after laser structuring. The influence of laser structuring on the day of structuring seems to be independent of the scan line distance. After 7 days, the contact angles increase until they reach their highest value after 21 days.

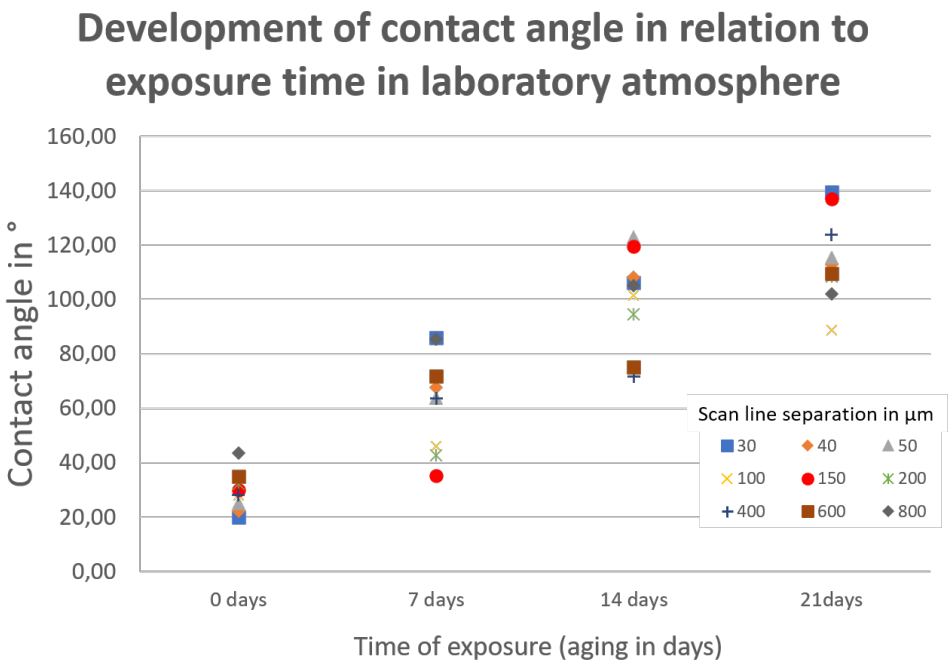

Fig. 9. Development of water contact angle in relation to exposure time in laboratory atmosphere and scan line separation of the laser structured samples

According to [Kietzig, A.M., 2019] the change in wetting properties is due to chemical surface modification in addition to laser structuring. The decomposition of carbon dioxide from the air into carbon and magnetite could be a possible cause for the increase in the contact angle. This statement needs further investigation.

4. Conclusions

We have managed to generate a water-repellent surface on stainless steel by ultra-short pulse laser processing in the nearly superhydrophobic state. For superhydrophobic surfaces, the contact angle to water must be extremely high (>150°) and have a very small contact angle hysteresis (<10°). The solid surface should have the lowest possible surface free energy. According to the Cassie-Baxter and Wenzel model, a structure in the micro- and nanometer range helps to reduce the contact area to the wetting liquid and thus to increase the Young's contact angle.

It seems that the aging of the laser structured surface leads to a chemical modification of it. The influence of the scan line separation shows a lower significance than aging itself both after the laser material processing and after aging.

Acknowledgements

The author thanks the Materials Research Institute Aalen, IMFAA for assistance with sample preparation. Furthermore, thanks to the working group of Laser Application Center, LAC and Institute for Innovative Surfaces, FINO for support and discussions.

References

Bhushan, B., 2018. Biomimetics, 3rd Edition, Springer Series in Materials Science, 279

Cassie, A.B.D., Baxter, S., 1944. Wettability of porous surface, Transactions of the Faraday Society, 40, p. 546-551

Deutsche Edelstahlwerke, 2015. Werkstoffdatenblatt X5CRNi18-10 – 1.4301

Deutsches Institut für Normung, DIN EN 828. Klebstoffe - Benetzbarkeit - Bestimmung durch Messung des Kontaktwinkels und der freien Oberflächenenergie fester Oberflächen. Klebstoffe - Benetzbarkeit - Bestimmung durch Messung des Kontaktwinkels und der freien Oberflächenenergie fester Oberflächen

Ghasemlou, M., Daver, F., Ivanova, E.P., Adhikari, B., 2018. Bio inspired sustainable and durarable superhydrophobic materials: from nature to market, Journal of Materials Chemistry, 7, p. 16643-16670

Gurera, D., Bhushan, B., Kumar, N., 2018. Lessons from mosquitoes' painless piercing, Journal of the mechanical bevior of biomedical materials, 84, p. 178-187

Kietzig, A.M., Hatzikiriakos, S.G., Englezos, P., 2009. Patterned superhydrophobic metallic surfaces, Langmuir, 25, p. 4821-4827

KRÜSS Scientific, 2017. Drop Shape Analyzer – DSA100 – User Manual, Version 2-17

Müller, F. A., Kunz, C. Gräf, S., 2016. Bio-inspired functional surfaces based on laser-induced perdiodic surface structure, Materials, 9, p. 476

Neuenschwander, B., Jaeggi B., Schmid, M., Rouffiange, V. Martin, P.E., 2012. Optimization of the volume ablation rate for metals at different laser pulse-durations from ps to fs, Laser Applications in Microelectronic and Optoelectronic Manufacturing, 8243

Nolte, S., Momma, C., Chichkov, B.N., Welling, H., 1999. Mikrostrukturierung mit ultrakurzen Laserpulsen, Physik Journal, 55, p. 41-44

Ta, V.D., Dunn, A., Wasley, T.J., Li, J. Kay, R.W., Stringer, J., Smith, P.J., Esenturk, E., Connaughton C., Shephard J.D., 2016. Laser textured superhydrophobic surfaces and their applications for homogenous spot deposition, Applied Surface Science, 365, p. 153-159

Vorobyev, A.Y., Guo, C., 2013. Direct femtosecond laser surface nano/microstructuring and its applications, Laser & Photonics Reviews, 7, p. 385-407

Wang, S., Jiang, L., 2007. Definition of Superhydrophobic Surfaces, Advanced Materials, 19, p. 3423-3424

Wenzel, R.N., 1936. Resistance of solid surfaces to wetting by water, Industrial and Engineering Chemistry, 28, p.988-994

Wu, P. H., Cheng, C. W., Chang, C.P., Wu, T.M., Wang, J.K., 2011. Fabrication of large-area hydrophobic surfaces with femtosecond-laser-structured molds, Journal of Micromechanics and Microengineering, 21, p. 115032